RSC Advances

PAPER

View Article Online
View Journal | View Issue

Cite this: *RSC Adv.*, 2021, **11**, 33276

Effects of external electric field on the sensing property of volatile organic compounds over Janus MoSSe monolayer: a first-principles investigation†

Chen-Hao Yeh, * Yu-Tang Chen and Dah-Wei Hsieh

Janus 2D transition metal dichalcogenide (TMD) is a new generation 2D material with a unique asymmetric structure. This asymmetric structure (or out-off plane symmetric geometry) of Janus 2D TMD has been reported to yield tunable electronic properties through strain and electric field, which can also be applied in gas sensing. In this work, we performed DFT calculations to investigate the gas sensing property of cyclohexane and acetone on MoS_2 and Janus MoSSe monolayers under external electric fields. Our results show that cyclohexane possesses slightly larger adsorption energy on pristine MoS_2 and Janus MoSSe monolayers than acetone without external electric fields. After applying the external electric fields, the adsorption energy for cyclohexane on MoS_2 shows no enhancement. However, the adsorption energy of acetone shows the most substantial enhancement on the Janus MoSSe monolayer. We found that the dipole moment orientations of adsorbates and the monolayer can strongly interact with the external electric fields. Hence, the combination of polar adsorbate and polar material, *i.e.*, acetone and Janus MoSSe, demonstrates the most vital sensitivity under the applied bias. On the other hand, the non-polar adsorbate and non-polar material combination show a negligible effect on external bias. These findings can be applied to the design of gas sensors in the future through polar materials.

Received 29th July 2021
Accepted 27th September 2021

DOI: 10.1039/d1ra05764b

rsc.li/rsc-advances

1. Introduction

Since the discovery of graphene, two-dimensional (2D) materials have gradually attracted significant attention due to their many unique properties, which are distinct from the 3D bulk materials.[1–9] Transition metal dichalcogenides (TMD) are one of the most widely studied 2D materials due to their specific electrical, optical, and other physical properties.[10–14] Recently, Janus 2D TMD materials have gradually attracted considerable interest and have two different atom layers on two sides to generate an out-off plane symmetry of its geometry. MoSSe, a single-layer Janus 2D TMD, has been successfully fabricated experimentally through the modified CVD method,[15,16] although Janus MoSSe does not exist in nature. Theoretically, the MoSSe monolayer has been demonstrated to be stable by calculating the phonon dispersion and through molecular dynamics simulations.[17] Compared with the traditional 2D TMD monolayers, Janus 2D TMD monolayers have many advantages based on their unique electronic properties, such as tunable bandgap, Rashba effect, and piezoelectric effect. In addition, it has been recently reported that Janus 2D TMD monolayers can be applied in many fields, including catalysts,[18] transistors,[19] optoelectronic devices,[20] and sensors.[21] Recently, there have been many studies regarding the gas sensing properties using the Janus 2D TMD monolayers. For example, using first-principle calculations, Janus MoSSe monolayers have been studied in the sensing NO_2, NH_3, SOF_6 decompositions species, adulterant compounds, and volatile organic compounds (VOCs).[22–28] In these reports, the sensing properties depend on electronic interactions and adsorption strength between the target gaseous molecules and the sensor materials. The enormous adsorption energy will lead to stronger sensitivity. Thus, it is crucial to enhance the sensitivity by increasing the adsorption energy of the gas molecules on Janus 2D TMD materials. In the literature, some studies have used chemical doping, strain deformation, and external electric fields to adjust the sensitivity of gas molecules.[29–32] Among these, strain deformation is commonly adopted, but external electric fields have been used in few studies for tuning the sensitivity of gas molecules on Janus 2D TMD monolayers.

It is well-known that the reactivity of catalytic reactions and the sensitivity of gas sensors can be modified by applying an external electric field.[33–37] In the literature, methane conversion reactions have been reported to show better catalytic activity over various catalysts under external electric fields than without applying external electric fields.[36,38,39] In addition, it has also been reported that 2D materials possess an excellent capability in capturing various gas molecules under external electric fields. For example, Sathishkumar *et al.* reported that the CO_2 adsorption energy could be significantly enhanced by applying

Department of Materials Science and Engineering, Feng Chia University, No. 100, Wenhwa Rd., Seatwen, Taichung, 40724, Taiwan. E-mail: chenhyeh@fcu.edu.tw

† Electronic supplementary information (ESI) available. See DOI: 10.1039/d1ra05764b

an external electric field on both N-doped penta-graphene and penta-C_2N nanosheets.[40,41] Moreover, Ma *et al.* calculated that the Sc_2CO_2 monolayer could regulate the adsorption strength of SO_2 by applying tensile strains or controlling external electronic fields.[42] Furthermore, for TMD materials, it has been reported that the external electric fields can significantly modulate charge transfer between the NO_2/NH_3 molecules and MoS_2.[43] However, the investigations on gas adsorption on Janus 2D TMD materials under external electronic fields are few, and the mechanism of external electronic fields towards gas adsorption on the Janus 2D TMD materials is also unknown. Thus, in this work, we investigated the adsorption and sensitivity of gas molecules on Janus 2D TMD materials under external electric fields.

Our previous studies have investigated that acetone possesses a good sensitivity over the Janus MoSSe monolayer.[26] Besides, it has been reported that external electric fields show high reactivity to polar gas molecules during their adsorption. Since acetone is a well-known polar gas molecule, we will study the adsorption of acetone on both Janus MoSSe and pristine MoS_2 monolayers under external electric fields. Moreover, we will also investigate the adsorption of another non-polar VOC, cyclohexane, on both Janus MoSSe and pristine MoS_2 monolayers under external electric fields for comparison.

2. Computational details

2.1 DFT calculations

All calculations were carried out using the Vienna Ab initio Simulation Package (VASP)[44–47] with the projector augmented wave (PAW) method.[48,49] The exchange–correlation functional adopted was the Perdew–Burke–Ernzerhof (PBE)[50] involved in the generalized gradient approximation (GGA) method. The Kohn–Sham orbitals were expanded in a plane-wave basis set with a kinetic energy cutoff of 520 eV. All calculations of 2D transition metal dichalcogenide monolayers were carried out using the 2H phase of pristine MoS_2 and Janus MoSSe. The (4×4) supercell is considered for all TMDs monolayers with 15 Å vacuum along the *c*-axis to avoid the interlayer interaction, as shown in Fig. 1. As dipole interactions are necessary, the dipole corrections perpendicular to all monolayers were carried out in the calculations. The Brillion zone were sampled using $(4 \times 4 \times 1)$ Gamma-centered Monkhorst–Pack *k*-points mesh[51] for VOCs adsorption on different TMDs. The convergence threshold was 1×10^{-5} eV for the total electronic energy in the self-consistent loop. The atomic positions were relaxed using the quasi-Newton algorithm until the *x*, *y*, and *z*-components of unconstrained atomic force were smaller than 1×10^{-2} eV Å^{-1}. The dispersion energy correction was considered using the DFT-D3 method by Grimme *et al.*[52,53] The density-derived electrostatic and chemical (DDEC6) approach was examined for the electron transfer between the molecule and surface to analyze the electrical properties.[54–56] Besides, the following equation defines the adsorption energies (E_{ads}) of VOCs on the TMDs monolayers:

$$E_{ads} = E_{VOC/TMD} - E_{VOC} - E_{TMD} \quad (1)$$

$E_{VOC/TMD}$ is the total energy of VOCs adsorbed on pristine MoS_2 or Janus MoSSe. E_{VOC} is the energy of free adsorbate VOC molecules, and E_{TMD} is the energy of pristine MoS_2 or Janus MoSSe monolayers.

2.2 External electric field calculations

The approach proposed by Neugebauer and Scheffler for adding the external electric field was used in this work. It generated an artificial dipole sheet at the middle of the vacuum space along the *z*-direction in the supercell to simulate a uniform electric field.[57] Besides, a large enough vacuum space is needed to avoid the overlap between the charge density of the slab and the artificial dipole sheet.[58] For an electron, it can tunnel to the vacuum when the distance between the surface and the artificial dipole sheet exceeds Φ/F (Φ and F are the work function and electric field, respectively). Since the calculated work functions of pristine MoS_2 and Janus MoSSe monolayers were 5.45 eV and 5.54 eV, respectively, the maximum width should be ~9 Å between the monolayers and the artificial dipole sheet under the maximum electric field ($F = 0.6$ V Å^{-1}). Furthermore, it is roughly expressed as $\exp(-\sqrt{\phi}z)$ for the charge density decaying, in which Φ is the work function (in eV), and *z* is the distance from the slab (in Å). Based on the calculated work function mentioned above, the charge density drops by order of magnitude per 0.90 Å. Thus, only negligible charge density resides around the dipole sheet introduced at ~9 Å. Moreover, if the vacuum thickness is too wide, the external electric field can pull out the electrons from the Fermi level of the surface to the vacuum to cause the field emissions.[58,59] In this work, because we set a ~18 Å vacuum space, the width between the monolayers and the dipole sheet is ~9 Å, which is enough to avoid the field emission issue. The above methods have been implemented in the VASP software, which can be realized by setting the keyword "EFIELD" in the INCAR during the calculation. Moreover, the dipole corrections to the slab and potential (IDIPOL and LDIPOL) should also be included in the calculation when applying external electric fields.

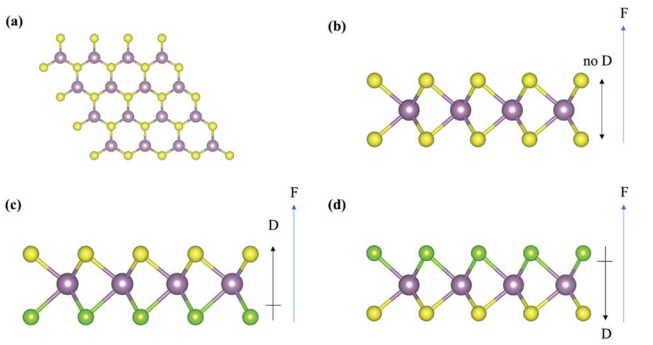

Fig. 1 (a) Top view of the optimized TMDs monolayers with the 2H phase, (b) side view of the MoS_2 monolayer under external electric field, (c) side view of the S-layer of MoSSe monolayer under external electric field, (d) side view of the Se-layer of MoSSe monolayer under external electric field. The *D* and *F* represent the intrinsic dipole moment of the monolayer as well as the external electric field, respectively, where the arrows indicate their directions. The purple, yellow, and green spheres represent Mo, S, and Se, respectively.

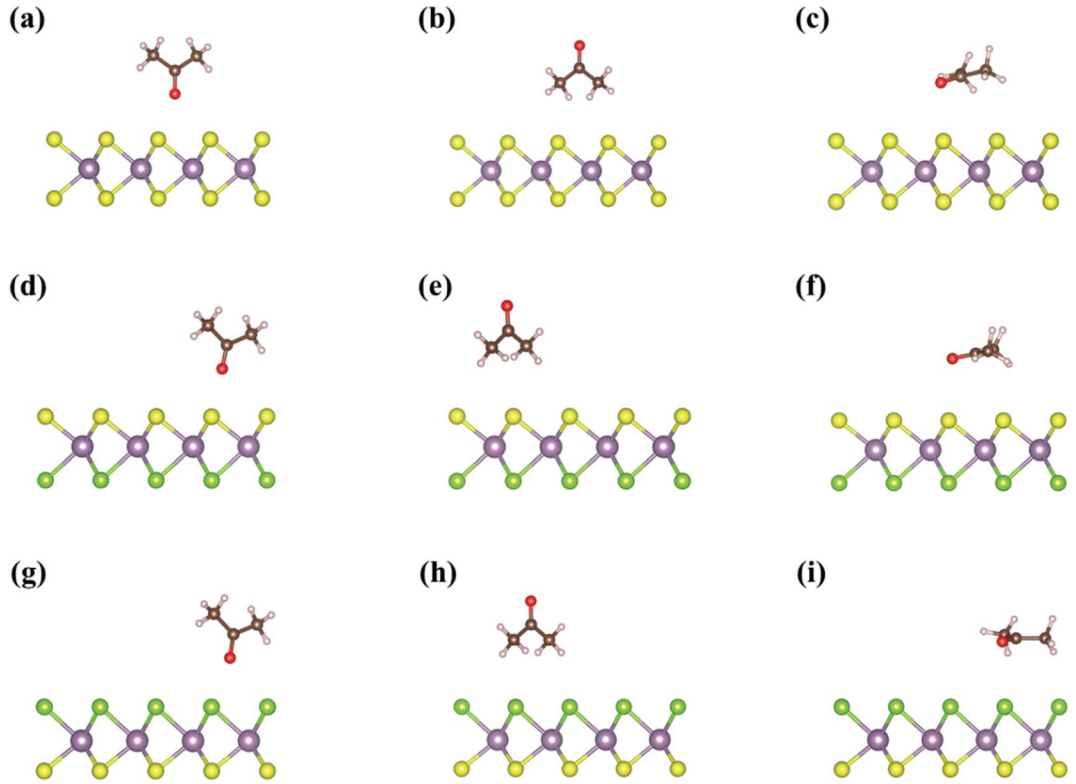

Fig. 2 Optimized adsorption structures of acetone on the TMDs monolayers without the external electric fields: (a) Ace_{v1}, (b) Ace_{v2}, and (c) Ace_h, on MoS_2; (d) Ace_{v1}, (e) Ace_{v2}, and (f) Ace_h, on S-layer of the Janus MoSSe; (g) Ace_{v1}, (h) Ace_{v2} and (i) Ace_h, on Se-layer of the Janus MoSSe. Purple, yellow, and green spheres represent Mo, S, and Se atoms, respectively, while brown, red, and light pink balls are C, O, and H atoms, respectively.

3. Results and discussion

3.1 Adsorption of acetone and cyclohexane on MoS_2 and Janus MoSSe monolayers without external electric fields

Fig. 2 shows three different adsorption structures of acetone on Janus MoSSe and MoS_2 monolayers without an external electric field. The adsorption structures of acetone can be divided into (1) acetone vertically adsorbing on the surface using its O end, named Ace_{v1}, (2) acetone vertically adsorbing on the surface using its C–H end, named Ace_{v2}, and (3) acetone adsorbing on the surface parallelly, named Ace_h. The adsorption energies of Ace_{v1}, Ace_{v2}, and Ace_h on pristine MoS_2 monolayer are −0.24 eV, −0.29 eV, and −0.36 eV, respectively. In addition, since the Janus MoSSe monolayer possesses an asymmetric structure on both sides, the acetone molecule can adsorb on either the S-layer or Se-layer using the adsorption configuration mentioned above. The adsorption energies of Ace_{v1}, Ace_{v2}, and Ace_h on the S-layer of the MoSSe monolayer are −0.22 eV, −0.29 eV, and −0.32 eV, respectively, while the adsorption energies of Ace_{v1}, Ace_{v2}, and Ace_h on the Se-layer of the MoSSe monolayer are −0.23 eV, −0.25 eV, and −0.35 eV, respectively. These results reveal that the parallel adsorption of acetone molecule is the most favorable adsorption structure on the TMD monolayers. We also calculated the adsorption of a non-polar VOC molecule, cyclohexane, on both pristine MoS_2 and Janus MoSSe monolayers in the absence of the external electric field. The most favorable adsorption structure of cyclohexane on the TMDs is also the parallel adsorption configuration using the van der Waals interaction, as shown in Fig. 3. The calculated adsorption energies of cyclohexane on pristine MoS_2, S-layer of

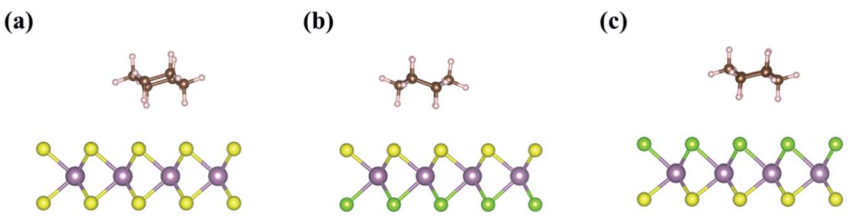

Fig. 3 Optimized adsorption structures of cyclohexane on the (a) MoS_2, (b) S-layer of the Janus MoSSe, and (c) Se-layer of the Janus MoSSe without the external electric fields. Purple, yellow, and green spheres represent Mo, S, and Se atoms, respectively, while brown, red, and light pink balls are C, O, and H atoms, respectively.

Table 1 The calculated adsorption energy, E_{ads} for different adsorption structures of acetone and cyclohexane on pristine MoS_2 and Janus MoSSe monolayers

TMD	Species	Adsorption type	E_{ads} (eV)
MoS_2		Ace_{v1}	−0.24
	Acetone	Ace_{v2}	−0.29
		Ace_h	−0.36
	Cyclohexane	Parallel	−0.39
MoSSe-S		Ace_{v1}	−0.22
	Acetone	Ace_{v2}	−0.29
		Ace_h	−0.32
	Cyclohexane	Parallel	−0.36
MoSSe-Se		Ace_{v1}	−0.23
	Acetone	Ace_{v2}	−0.25
		Ace_h	−0.35
	Cyclohexane	Parallel	−0.37

MoSSe, and Se-layer of MoSSe monolayers are −0.39 eV, −0.36 eV, and −0.37 eV, respectively. The adsorption energy of cyclohexane on the 2D TMDs is slightly larger than that of acetone (Table 1).

3.2 Adsorption of acetone on MoS_2 monolayer with external electric fields

Subsequently, we investigated the adsorption of acetone on a pristine MoS_2 monolayer in the presence of external electric fields, as shown in Fig. 4. The magnitude of external electric fields applied was between −0.6 V Å^{-1} to +0.6 V Å^{-1}. As mentioned above, three possible adsorption structures are also listed out for acetone adsorption on pristine MoS_2. As shown in Table 2, in the presence of the external electric field of +0.6 V Å^{-1}, we found that the adsorption energy of Ace_{v1}, Ace_{v2}, and Ace_h on the pristine MoS_2 monolayer becomes 0.28 eV, −0.49 eV, and −0.17 eV, respectively. It shows that the adsorption energy of Ace_{v2} increases while that of Ace_{v1} and Ace_h decreases in comparison with that in the absence of the external electric field. Besides, in the presence of external electric fields of +0.4 and +0.2 V Å^{-1}, we observe similar trends, in which the adsorption energy of Ace_{v2} still increases and those for Ace_{v1} and Ace_h decrease, as listed in Table 2. The result indicates that the adsorption energy of Ace_{v2} is enhanced by the favorable external electric field, whereas that of Ace_{v1} and Ace_h are weakened, especially for Ace_{v1}, under the positive bias.

On the other hand, when applying negative external electric fields of −0.60 V Å^{-1}, −0.40 V Å^{-1}, and −0.20 V Å^{-1}, the adsorption energy of Ace_{v1} on the pristine MoS_2 monolayer becomes −0.50 eV, −0.52 eV, and −0.38 eV, respectively. However, the adsorption energy of Ace_{v2} on pristine MoS_2 monolayer becomes 0.18 eV, −0.06 eV, and −0.17 eV in the presence of external electric fields of −0.6 V Å^{-1}, −0.4 V Å^{-1}, and −0.2 V Å^{-1}, respectively. Interestingly, the adsorption energy of Ace_{v1} on pristine MoS_2 monolayer is enhanced by the negative external electric field, which shows the opposite trend to the results of applying positive external electric fields.

3.3 Adsorption of acetone on Janus MoSSe monolayer with external electric fields

For the adsorption of acetone on the Janus MoSSe monolayer in the presence of external electric fields, we found that the S-layer and Se-layer of Janus MoSSe show extreme differences. Fig. 5 displays all the adsorption structures of acetone on the Janus MoSSe monolayer under positive or negative external electric fields. First, on the S-layer of Janus MoSSe monolayer (Fig. 5(a)–

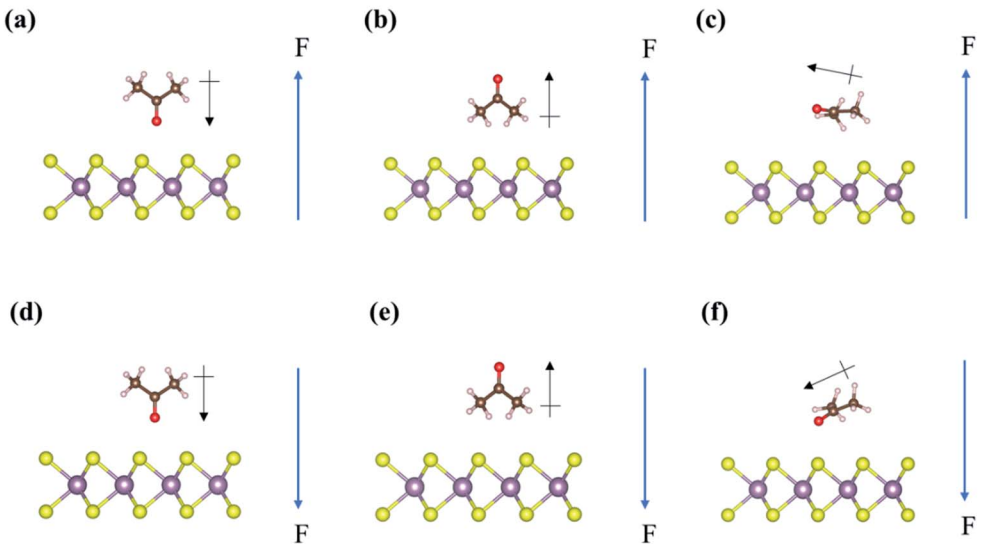

Fig. 4 Optimized adsorption structures of acetone on MoS_2 in the presence of the external electric field: (a) Ace_{v1}, (b) Ace_{v2}, and (c) Ace_h under the positive external electric field; (d) Ace_{v1}, (e) Ace_{v2}, and (f) Ace_h under the negative external electric field. The arrows are the directions of the dipole moment and the external electric field. Purple and yellow spheres represent Mo and S atoms, respectively, while brown, red, and light pink balls are C, O, and H atoms, respectively.

Table 2 Summary of electric field effects on the calculated adsorption energy, E_{ads}, for different adsorption structures of acetone on pristine MoS_2 and Janus MoSSe monolayers

E-field strength (V Å^{-1})	MoS_2			MoSSe-S			MoSSe-Se		
	Ace_{v1}	Ace_{v2}	Ace_h	Ace_{v1}	Ace_{v2}	Ace_h	Ace_{v1}	Ace_{v2}	Ace_h
0.6	0.28	−0.49	−0.17	−0.05	−0.85	−0.50	0.57	0.21	−0.11
0.4	0.02	−0.52	−0.31	−0.20	−0.77	−0.55	0.26	−0.10	−0.26
0.2	−0.11	−0.40	−0.34	−0.21	−0.53	−0.42	0.02	−0.20	−0.26
0	−0.24	−0.29	−0.36	−0.22	−0.29	−0.32	−0.23	−0.25	−0.35
−0.2	−0.39	−0.17	−0.38	−0.23	−0.05	−0.24	−0.48	−0.26	−0.50
−0.4	−0.52	−0.06	−0.44	−0.25	0.17	−0.19	−0.74	−0.27	−0.66
−0.6	−0.50	0.18	−0.36	−0.11	0.51	0.03	−0.84	−0.13	−0.65

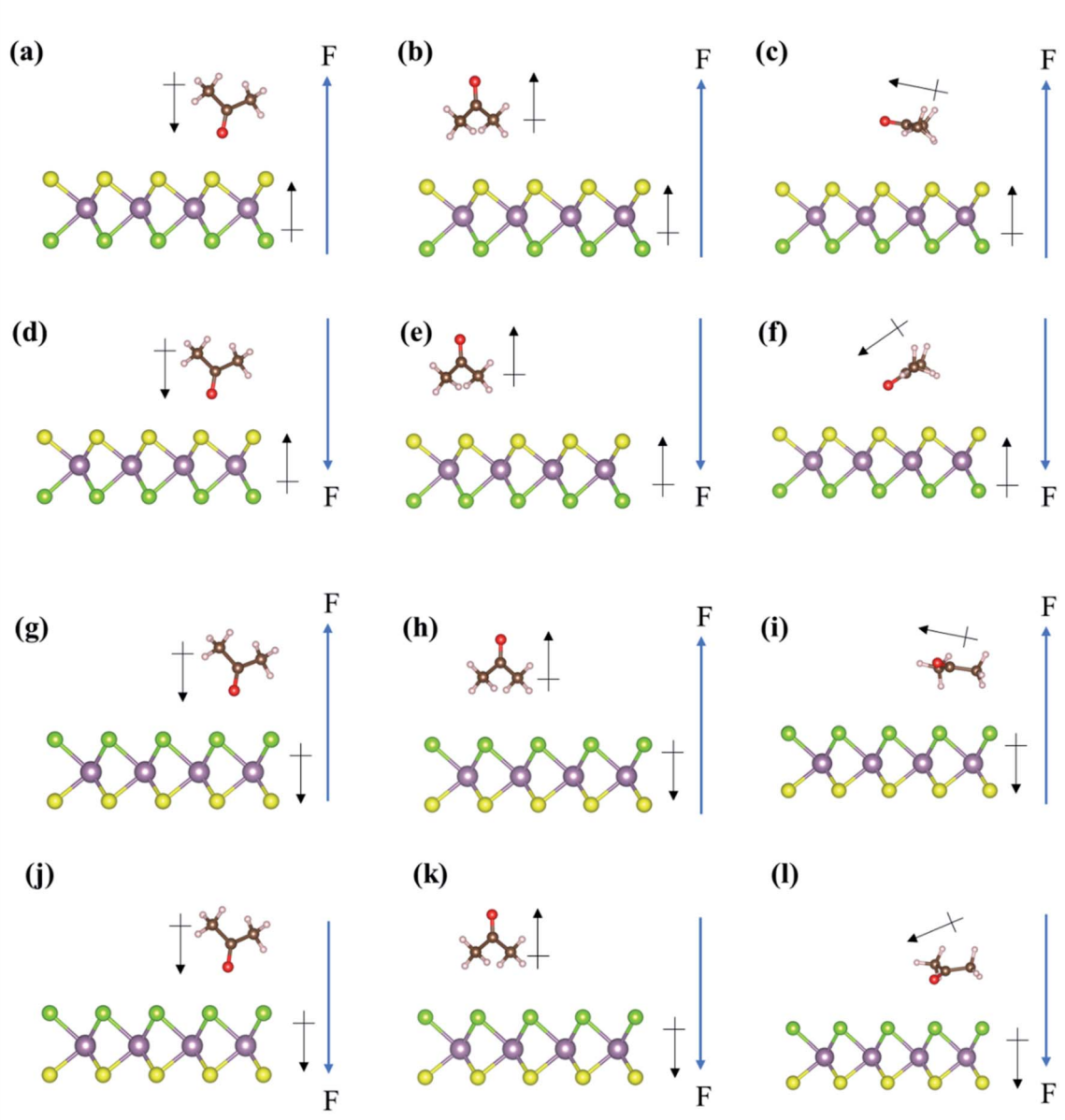

Fig. 5 (a) Ace_{v1}, (b) Ace_{v2}, and (c) Ace_h under a positive external electric field; (d) Ace_{v1}, (e) Ace_{v2}, and (f) Ace_h under a negative external electric field, in the optimized adsorption structures of acetone on the S-layer of Janus MoSSe. (g) Ace_{v1}, (h) Ace_{v2}, and (i) Ace_h under the positive external electric field; (j) Ace_{v1}, (k) Ace_{v2}, and (l) Ace_h under the negative external electric field, in the optimized adsorption structures of acetone on the Se-layer of Janus MoSSe. The arrows are the directions of the dipole moment and the external electric field. Purple, yellow, and green spheres represent Mo, S, and Se atoms, respectively, while brown, red, and light pink balls are C, O, and H atoms, respectively.

(f)), the adsorption energy of Ace_{v1} is −0.21 eV, −0.20 eV, and −0.05 eV under +0.2 V Å^{-1} to +0.6 V Å^{-1}, while it is −0.23 eV, −0.25 eV, and −0.11 eV under −0.2 V Å^{-1} to −0.6 V Å^{-1}, respectively. This result reveals that the adsorption energy of Ace_{v1} almost remains at around −0.23 eV and then decreases after the external electric fields increases to +0.6 V Å^{-1} or −0.6 V Å^{-1}. On the contrary, the adsorption energy of Ace_{v2} on the S-layer of Janus MoSSe monolayer increases to −0.53 eV, −0.77 eV, and −0.85 eV under the external electric fields of +0.2 V Å^{-1}, +0.4 V Å^{-1}, and +0.6 V Å^{-1}, respectively. However, the adsorption energy of Ace_{v2} dramatically decreases to −0.05, 0.17, and 0.51 eV from −0.2 V Å^{-1} to −0.6 V Å^{-1}, respectively. Besides, the adsorption energy of Ace_h possesses similar changing trends to Ace_{v2} in that the positive bias can enhance its adsorption energy. However, the negative bias will inhibit the adsorption energy of Ace_h on the S-layer of the Janus MoSSe monolayer.

Moreover, the adsorption structures of Ace_h will be orientated by the positive bias and then tilt around 30° (Fig. 5(c)). In comparison, the negative bias can result in a tilting angle of about −30° in the adsorption structure of Ace_h on the S-layer of Janus MoSSe monolayer (Fig. 5(f)). Our results demonstrate that either positive or negative external electric fields show immense magnitude change to Ace_{v2} and Ace_h on the S-layer of Janus MoSSe monolayer, particularly for Ace_{v2}. However, the effect of external electric fields on Ace_{v1} is limited. Hence, the adsorption energy of acetone in the presence of the external electric field on the S-layer of the Janus MoSSe monolayer displays a different trend to that on the pristine MoS_2 monolayer.

On the Se-layer of the Janus MoSSe monolayer, the adsorption energy of acetone shows an opposite trend to the counterpart of acetone on the Janus MoSSe monolayer's S-layer in Fig. 5(g)–(l). The adsorption energy of Ace_{v1} on the Se-layer of the Janus MoSSe monolayer dramatically changes in a range from 0.57 eV to −0.84 eV under +0.6 V Å^{-1} to −0.6V Å^{-1}, which is similar to the changing magnitude of Ace_{v2} on the S-layer of the Janus MoSSe monolayer. Likewise, as listed in Table 2, the changing magnitude of the adsorption energy for Ace_{v2} on the Se-layer of the Janus MoSSe monolayer is like the trend of Ace_{v1} on the S-layer of the Janus MoSSe monolayer. Furthermore, the positive external electric field shows an inhibition to the adsorption energy for Ace_h. In contrast, the negative external electric field demonstrates the enhancement of the adsorption energy of Ace_h on the Se-layer of the Janus MoSSe monolayer. This result is opposite to the adsorption of Ace_h on the S-layer of the Janus MoSSe monolayer. Consequently, we found that external electric fields substantially affect the adsorption energy of Ace_{v1} and Ace_h on the Se-layer of Janus MoSSe monolayer, particularly for Ace_{v1}. In summary, the result indicates that the Janus MoSSe monolayer shows highly selective sensitivity concerning the acetone molecule in the presence of external electric fields.

3.4 Adsorption of cyclohexane on Janus MoSSe and MoS_2 monolayers with external electric fields

The adsorption of cyclohexane on the Janus MoSSe monolayer represents the interaction between a non-polar molecule and a polar material, as shown in Fig. 6. In the presence of external electric fields, the adsorption energy of cyclohexane on the S-

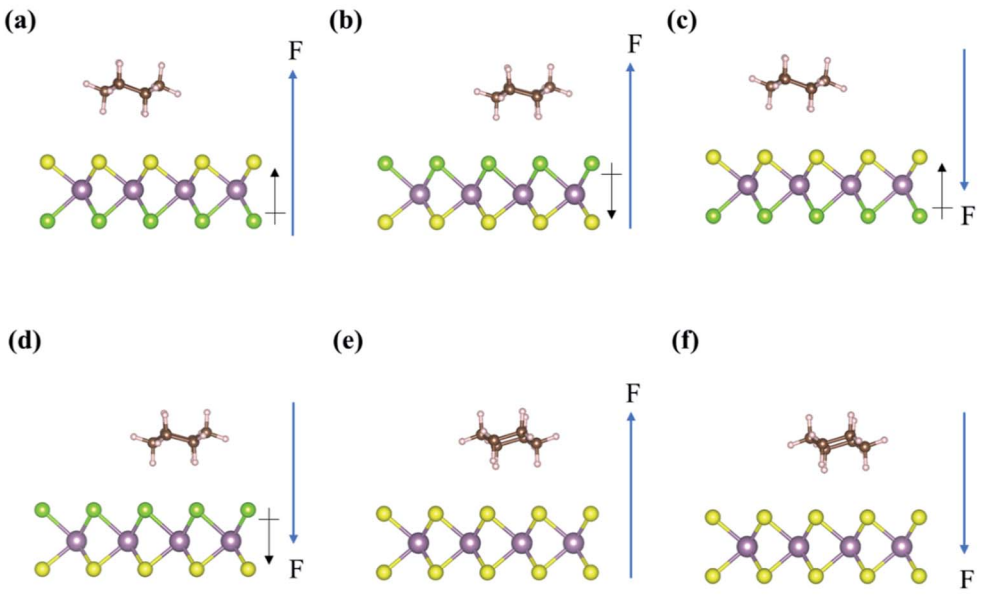

Fig. 6 Optimized adsorption structures of cyclohexane on the (a) S-layer of Janus MoSSe with the positive external electric field, (b) Se-layer of Janus MoSSe with the positive external electric field, (c) S-layer of Janus MoSSe with the negative external electric field, (d) Se-layer of Janus MoSSe with the negative external electric field, (e) MoS_2 with the positive external electric field, and (f) MoS_2 with a negative external electric field. The arrows are the directions of the dipole moment and the external electric field. Purple, yellow, and green spheres represent Mo, S, and Se atoms, respectively, while brown, red, and light pink balls are C, O, and H atoms, respectively.

Table 3 Summary of electric field effects on the calculated adsorption energy, E_{ads}, for different adsorption structures of cyclohexane on pristine MoS_2 and Janus MoSSe monolayers

E-field strength (V Å^{-1})	Cyclohexane		
	MoS_2	MoSSe-S	MoSSe-Se
0.6	−0.38	−0.72	0.00
0.4	−0.39	−0.60	−0.10
0.2	−0.39	−0.48	−0.22
0	−0.39	−0.36	−0.37
−0.2	−0.39	−0.24	−0.46
−0.4	−0.40	−0.12	−0.58
−0.6	−0.40	−0.01	−0.72

layer of the Janus MoSSe monolayer becomes −0.72 eV, −0.60 eV, −0.48 eV, −0.24 eV, −0.12 eV, and −0.01 eV, under the external electric field values from +0.6 V Å^{-1} to −0.6 V Å^{-1}, as listed in Table 3. In addition, the adsorption energy of cyclohexane on Se-layer of the Janus MoSSe monolayer illustrates an inverse result. The adsorption energy varies from −0.01 eV to −0.72 eV when the external electric field is from +0.6 V Å^{-1} to −0.6 V Å^{-1}. Furthermore, the adsorption energy of cyclohexane on pristine MoS_2 monolayer almost remains constant at around −0.39 eV under either positive or negative external electric fields. Compared with cyclohexane adsorption on pristine MoS_2 monolayer, the Janus MoSSe monolayer shows better sensitivity than the MoS_2 monolayer under external electric fields (MoS_2 monolayer shows no change in the adsorption energy under external electric fields). Moreover, we observe that the changing trends in the adsorption energies of cyclohexane are the same at both sides of the Janus MoSSe monolayer, and the only difference is the direction of external electric fields.

3.5 Dipole moment analysis

Our results find that both acetone and cyclohexane show good sensitivity on the Janus MoSSe monolayer in the presence of external electric fields. However, only the acetone molecule is affected by external electric fields on the pristine MoS_2 monolayer. Moreover, the changing magnitude of the adsorption energy of acetone on the Janus MoSSe monolayer is much stronger than that on the MoS_2 monolayer. As mentioned in the previous studies,[34,36] the external electric fields can couple with the internal electric fields between the gas molecule and surface and the intrinsic dipole moments of the gas molecule. In this study, since both acetone and Janus MoSSe monolayer possess intrinsic dipole moments, the external electric fields could interact with both of them. Hence, we observed that the directions of intrinsic dipole moments of acetone and MoSSe monolayer strongly correlate with the directions of external electric fields. In VASP software, the directions of positive and negative external electric fields were set as upward (↑) and downward (↓), respectively. Therefore, when the directions of the external electric field and dipole moments are in the same direction, the adsorption energy of acetone has the most prominent enhancement. This situation occurs in the adsorption of Ace_{v2} on the S-layer (see the arrows in Fig. 5(b)) and Ace_{v1} on the Se-layer (see the arrows in Fig. 5(j)) of the MoSSe monolayer under positive and negative external electric fields, respectively. Second, when one of the dipole moments in either acetone or Janus MoSSe is opposite to the external electric fields, the adsorption energy of acetone will decrease, as shown by the arrows in Fig. 5(a), (d), (h), and (k).

Furthermore, when the direction of the external electric field is opposite to both acetone and MoSSe monolayer, the adsorption energy of acetone will dramatically and remarkably decrease, even the positive adsorption energy value, for instance, the Ace_{v2} on the S-layer of the Janus MoSSe monolayer under negative external electric field (Fig. 5(e)), or the Ace_{v1} on the Se-layer of the Janus MoSSe monolayer under positive external electric field (Fig. 5(g)). All the detailed orientations of adsorbates, surfaces, and external electric fields are recorded in Tables S1 and S2.†

Similarly, in the adsorption of cyclohexane on the Janus MoSSe monolayer under an external electric field, the external electric field can only react with the intrinsic dipole moment of the MoSSe monolayer since cyclohexane has no dipole moment. Hence, the change in the adsorption energy of cyclohexane on the Janus MoSSe monolayer is only altered by the direction between the intrinsic dipole moment of the MoSSe monolayer and the external electric field. The positive external electric field can enhance the adsorption energy of cyclohexane on the S-layer of the MoSSe monolayer. In contrast, the negative external electric field can enhance the adsorption energy of cyclohexane on the Se-layer of MoSSe monolayer and *vice versa*, as listed in Table S3.†

A similar phenomenon is also observed in the adsorption of acetone and cyclohexane on the MoS_2 monolayer, as shown by the arrows in Fig. 4 and 6. For the adsorption of acetone on MoS_2, since only acetone has the intrinsic dipole moment, it can enhance the adsorption energy of acetone when the direction of its intrinsic dipole moment and the external electric field are the same and *vice versa*, as listed in Tables S1 and S2.† For the adsorption of cyclohexane on the MoS_2 monolayer, because both cyclohexane and MoS_2 monolayer have no intrinsic dipole moment, the adsorption energy can not be altered by the external electric field, as shown in Table S3.†

3.6 Sensing of NO molecule

In the literature, it has been reported that both MoSSe and MoS_2 monolayers possess good sensitivity towards smaller and simpler toxic species, such as NO molecules.[22,43,60] Hence, we have calculated the NO sensing properties on both MoSSe and MoS_2 monolayers in the presence of external electric fields. NO molecule possesses a small dipole moment value of 0.16 D, while the dipole moment value of the MoSSe monolayer is 2.99 D. Thus, the external electric field can majorly react with the intrinsic dipole moment of the MoSSe monolayer when NO adsorbs on the MoSSe monolayer under the external electric field. The adsorption energies of NO on the MoSSe monolayer majorly depend on the orientations between the MoSSe

monolayer and the external electric field. When the orientations between the MoSSe monolayer and the external electric field are the same, the adsorption energies of NO on the MoSSe monolayer can be enhanced and *vice versa*, as shown in Fig. S1 and Table S4.† Moreover, the adsorption energies of NO on the MoS_2 monolayer change only slightly with and without the external electric fields. It results from the small dipole moment value of the NO molecule since the MoS_2 monolayer is a non-polar material. However, although the MoSSe monolayer also has better sensitivity towards NO sensing under external electric fields, the adsorption energies of the NO molecule are still smaller than that of acetone and cyclohexane on the MoSSe monolayer.

3.7 Electronic property analysis

As mentioned earlier, the adsorption structures of both Ace_{v1} and Ace_{v2} can be strongly regulated by different orientations of external electric fields on the Janus MoSSe monolayer. The adsorption energy of Ace_{v1} on the Se-layer of MoSSe can be enhanced by the negative bias, while that of Ace_{v2} on the S-layer of MoSSe can be enhanced by the positive bias. Therefore, we calculate the net atomic charges by DDEC6 of acetone on the Janus MoSSe monolayer to further understand the interaction between the external electric fields and the electron transfer of the gas/surface, as listed in Table 4. We considered the DDEC6 charges for Ace_{v1} on the Se-layer of MoSSe and Ace_{v2} on the S-layer of MoSSe. Without the external electric field, the calculated DDEC6 charge of Ace_{v1} on the Se-layer of MoSSe is $0.074|e|$, indicating that the electron transfer is from acetone to the Se-layer MoSSe. This electron transfer also represents that the direction of the internal electric field between Ace_{v1} and Se-layer of MoSSe is downward. When applying the negative external electric field in the same direction, the internal electric field between Ace_{v1} and the Se-layer of MoSSe can be enhanced by the external electric field. Hence, the electron transfer between Ace_{v1} on the Se-layer of MoSSe becomes $0.090|e|$, $0.105|e|$, and $0.122|e|$ under the external electric fields of -0.2 V Å^{-1}, -0.4 V Å^{-1}, and -0.6 V Å^{-1}, respectively. This result reveals that Ace_{v1} can donate more electrons to the Se-layer of MoSSe *via* enhancing the negative external electric field.

Table 4 Calculated DDEC atomic charges for the selected adsorption structures of acetone molecule after adsorption on Janus MoSSe monolayer. The positive and negative values indicate losing and gaining electrons of the acetone molecule

E-field strength (V Å^{-1})	TMD	Adsorption type	DDEC ($\|e\|$)
0.6	MoSSe-S	Ace_{v2}	-0.007
0.4	MoSSe-S	Ace_{v2}	0.008
0.2	MoSSe-S	Ace_{v2}	0.017
0	MoSSe-S	Ace_{v2}	0.033
0	MoSSe-Se	Ace_{v1}	0.074
-0.2	MoSSe-Se	Ace_{v1}	0.090
-0.4	MoSSe-Se	Ace_{v1}	0.105
-0.6	MoSSe-Se	Ace_{v1}	0.122

On the other hand, for the adsorption of Ace_{v2} and the S-layer of MoSSe, the calculated DDEC6 charge of Ace_{v2} is $0.033|e|$ in the absence of the external electric field. It also indicates that the electron transfer is from acetone to the S-layer of MoSSe. However, a positive external electric field can induce the electron transfer from the S-layer of MoSSe to acetone. Thus, as shown in Table 4, the calculated DDEC6 charges of Ace_{v2} become $0.017|e|$, $0.008|e|$, and $-0.007|e|$ under the external electric fields of +0.2 V Å^{-1}, +0.4 V Å^{-1}, and +0.6 V Å^{-1}, respectively. We found that the electron transfer between the S-layer of MoSSe and acetone changes from positive net charges to negative net charges, indicating that acetone transforms from being an electron donor to an electron acceptor with increasing external electric fields. These results demonstrate that the internal electric field between acetone and the MoSSe monolayer will also be strongly affected by external electric fields.

Besides, in our results, the DDEC6 charges of S and Se in MoS_2 and Janus MoSSe monolayers have different distributions under different external electric fields. For instance, the DDEC6 charges of S and Se in Janus MoSSe monolayer without electric field are $-0.239|e|$ and $-0.180|e|$, respectively. Under the electric field of +0.6 V Å^{-1}, the DDEC6 charges of S and Se in Janus MoSSe monolayer become $-0.274|e|$ and $-0.141|e|$, respectively. One can see that the net charge difference between S and Se increased from $0.059|e|$ to $0.133|e|$. This result indicates that the intrinsic dipole moment of Janus MoSSe can be enlarged by applying the external electric field.

3.8 Effective dipole moment and effective polarizability analysis

The relationship between the adsorption energy and dipole moment as well as polarizability in the presence of a uniform electric field could be summarized by a Taylor series as follows,[59,61–63]

$$E_{ads} = E^0_{ads} - \Delta\mu_{F=0}F - \frac{1}{2}\Delta\alpha_{F=0}F^2 + \ldots$$

E_{ads} and E^0_{ads} represent the approximated adsorption energies in the presence and the absence of an electric field, respectively. F is the magnitude of the external electric field. $\Delta\mu_{F=0}$ and $\Delta\alpha_{F=0}$ are the effective dipole moment difference and effective polarizability difference between the adsorbates and surfaces at the zero-electric field, respectively. Fig. 7 shows the plots of adsorption energies for acetone and cyclohexane on both pristine MoS_2 and Janus MoSSe monolayers as a function of external electric fields. Table 5 lists the fitting results from Fig. 7, which includes the effective dipole moment and effective polarizability for the adsorption of gas molecules on both pristine MoS_2 and Janus MoSSe monolayers.

We found that the effective polarizability of acetone on pristine MoS_2 varies from -0.56 to -0.80. In comparison, the effective polarizability of acetone on both sides of MoSSe displays a wide range from 0.08 to -1.66. This result implies that the effective polarizability change is more sensitive to acetone on MoSSe than on the MoS_2 monolayer. In addition, the absolute maximum

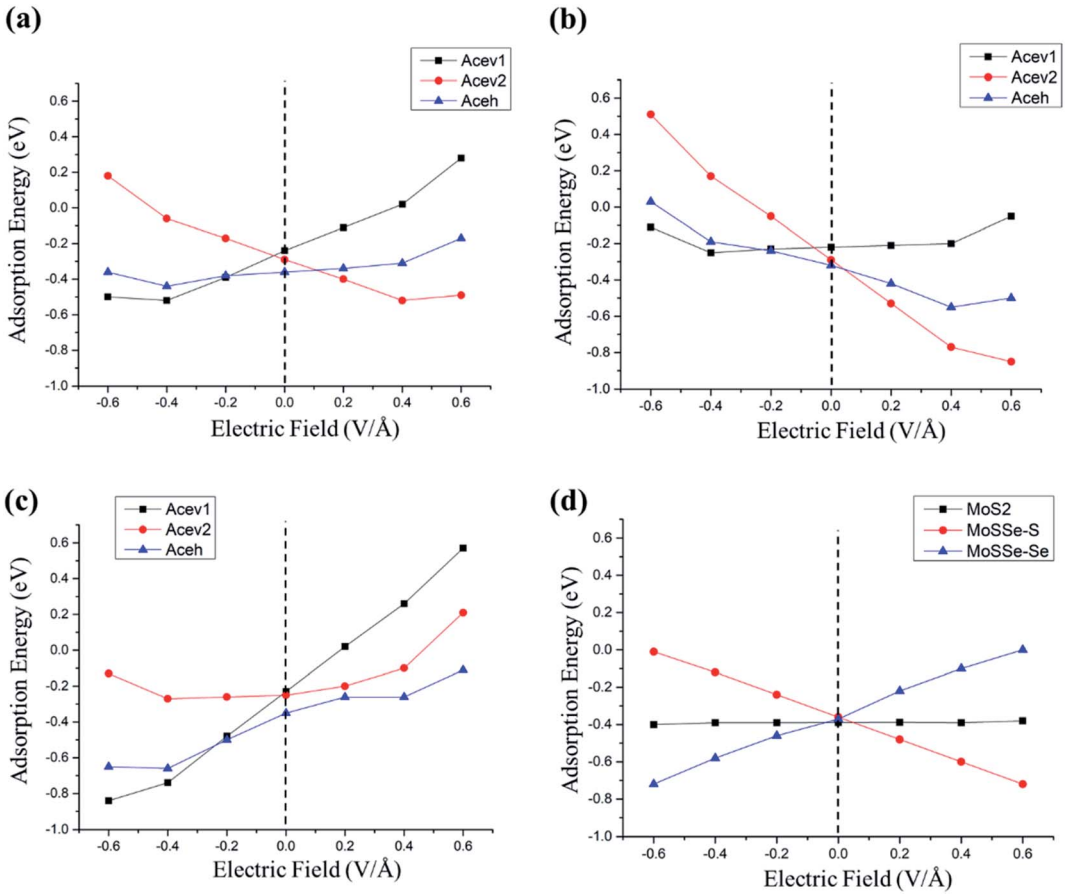

Fig. 7 Effects of an applied external electric field for (a) acetone on MoS_2, (b) acetone on the S-layer of Janus MoSSe, (c) acetone on the Se-layer of Janus MoSSe, and (d) cyclohexane on both MoS_2 and Janus MoSSe monolayers.

effective dipole moment of acetone on pristine MoS_2 is 0.66. In contrast, the corresponding value for acetone on Janus MoSSe is 1.20, almost two times that of acetone on MoS_2. Thus, the adsorption energy of a polar molecule on a polar material is more sensitive than that of a polar molecule on a non-polar material in the presence of an external electric field due to effective dipole moment and effective polarizability.

On the other hand, the effective polarizability of cyclohexane on both pristine MoS_2 and Janus MoSSe monolayer is negligible, which is in a range from 0.004 to 0.08. Moreover, the effective dipole moment of cyclohexane on pristine MoS_2 is also negligible, which is −0.01. However, the effective dipole moment of cyclohexane on Janus MoSSe monolayer possesses a value of −0.60. These results indicate that the external electric

Table 5 Fitting results of variations in the adsorption energies as a function of the electric field (V $Å^{-1}$) for acetone and cyclohexane adsorption on pristine MoS_2 and Janus MoSSe monolayers. $\Delta\mu_{F=0}$ and $\Delta\alpha_{F=0}$ are the corresponding calculated electric dipole moment (in e Å) and electric polarizability (in e $Å^2$ V^{-1}), respectively

TMD	Species	Adsorption type	Fitting results	$\Delta\mu_{F=0}$	$\Delta\alpha_{F=0}$
MoS_2		Ace_{v1}	$E_{ads} = -0.27 + 0.66F + 0.40F^2$	−0.66	−0.80
	Acetone	Ace_{v2}	$E_{ads} = -0.31 - 0.56F + 0.39F^2$	0.56	−0.78
		Ace_h	$E_{ads} = -0.38 + 0.15F + 0.28F^2$	−0.15	−0.56
	Cyclohexane	Parallel	$E_{ads} = -0.39 + 0.01F - 0.002F^2$	−0.01	0.004
MoSSe-S		Ace_{v1}	$E_{ads} = -0.25 + 0.05F + 0.42F^2$	−0.05	−0.84
	Acetone	Ace_{v2}	$E_{ads} = -0.32 - 1.15F + 0.36F^2$	1.15	−0.72
		Ace_h	$E_{ads} = -0.36 - 0.44F + 0.27F^2$	0.44	−0.54
	Cyclohexane	Parallel	$E_{ads} = -0.36 - 0.59F - 0.02F^2$	0.59	0.04
MoSSe-Se		Ace_{v1}	$E_{ads} = -0.25 + 1.20F + 0.28F^2$	−1.20	−0.56
	Acetone	Ace_{v2}	$E_{ads} = -0.28 + 0.25F + 0.83F^2$	−0.25	−1.66
		Ace_h	$E_{ads} = -0.39 + 0.48F - 0.04F^2$	−0.48	0.08
	Cyclohexane	Parallel	$E_{ads} = -0.35 + 0.60F - 0.02F^2$	−0.60	0.04

field can affect the effective dipole moment between cyclohexane and the Janus MoSSe monolayer. However, it does not affect the effective polarizability between cyclohexane and the Janus MoSSe monolayer. As a result, it is demonstrated that the adsorption energy of a non-polar molecule on a polar material could be strongly altered by an external electric field than that of a non-polar molecule on a non-polar material based on effective dipole moments.

3.9 Desorption temperatures analysis

To understand the desorption temperatures towards re-use of the sensor, we performed micro-kinetics simulations and calculated the desorption temperatures of adsorbates under different external electric fields. The MKMCXX software was used to calculate the microkinetic simulations.[64] Fig. S2(a)† illustrates the temperature evolution of acetone coverage on Janus MoSSe monolayer. Without applying the external electric fields, the desorption temperature of acetone on the MoSSe monolayer is from 150 K to 220 K. When increasing the magnitudes of the external electric fields, the desorption temperatures of acetone on the MoSSe monolayer also increase due to the enhancement of its adsorption energy. At 0.6 V $Å^{-1}$, the desorption temperature of acetone on the MoSSe monolayer is from 380 K to 500 K. Fig. S2(b) to (d)† show the calculated temperature-programmed desorption diagrams of acetone on MoS_2, cyclohexane on MoSSe, and cyclohexane on MoS_2 under different external electric fields, respectively. The results reveal that the desorption temperatures of acetone and cyclohexane on the MoSSe monolayer are located at a specific temperature under specific external electric fields, including high and low temperatures. On the other hand, the desorption temperatures of acetone and cyclohexane on the MoS_2 monolayer are all concentrated in the range of around 200 to 350 K. Thus, the calculated desorption temperatures demonstrate that the MoSSe monolayer can detect gas molecules at different specific external electric fields. It also reflects that the MoSSe monolayer possesses more sensitivity towards the detection of gas molecules under external electric fields. Besides, the mechanism for the gas molecule's desorption depends on the magnitudes of external electric fields as well as the desorption temperatures. A larger external electric field can lead to a higher desorption temperature and *vice versa*. Thus, tuning the external electric field can control the sensitivity of the sensor, and it can enable the re-use of the sensor.

4. Conclusions

We have employed DFT calculations to study the adsorption of acetone and cyclohexane on pristine MoS_2 and Janus MoSSe monolayers in the presence of external electric fields in this work. According to our results, cyclohexane shows slightly larger adsorption energy on both pristine MoS_2 and Janus MoSSe monolayers than that of acetone in the absence of external electric fields. In addition, under external electric fields, we found that the adsorption energy of acetone can be enhanced from −0.31 eV to −0.85 eV while that of cyclohexane can be enhanced from −0.36 eV to −0.72 eV on Janus MoSSe monolayer. Moreover, the adsorption energy of acetone on pristine MoS_2 monolayer also shows an enhancement from −0.35 eV to −0.57 eV in the presence of external electric fields. However, we observed that the adsorption energy of cyclohexane has almost no change on pristine MoS_2 monolayer in the presence of external electric fields.

To elucidate, we analyzed the dipole moments and the electron transfer between the adsorbates and the monolayers. Because the Janus MoSSe and acetone are polar species while pristine MoS_2 and cyclohexane are non-polar species, the intrinsic dipole moments of Janus MoSSe and acetone can react with the external electric fields. We found that when the orientations of dipole moments of Janus MoSSe, acetone, and external electric fields are all the same, this situation will maximize the adsorption energy of the acetone molecule. Besides, when there is only one polar species in the system, *i.e.*, acetone on MoS_2 or cyclohexane on Janus MoSSe, the enhancement of the adsorption energy for these gas molecules is smaller than the counterpart of acetone on Janus MoSSe. Finally, since cyclohexane and MoS_2 are without intrinsic dipole moments, the adsorption of cyclohexane on MoS_2 is not affected by the external electric fields. The calculated DDEC atomic charges also reveal that the internal electric field between acetone and Janus MoSSe will be enhanced or inhibited by external electric fields in different directions. By calculating the effective dipole moment and effective polarizability, we observe that the effective dipole moment plays an important role in the adsorption of either acetone or cyclohexane on Janus MoSSe monolayer under external electric fields. Consequently, our results demonstrate that polar materials possess better electric sensitivity than non-polar materials in the presence of external electric fields. This finding can be applied in the design of gas sensors and can be used in gas storage applications in the future through polar materials.

Conflicts of interest

There are no conflicts to declare.

Acknowledgements

The authors gratefully acknowledge the financial support for this work from the grant 109-2113-M-035-003-MY3 of the Ministry of Science and Technology (MOST), Taiwan. The National Center of High-Performance Computing (NCHC) contributed to this project by allowing access to their computer facilities and donating computer time.

References

1 K. S. Novoselov, A. K. Geim, S. V. Morozov, D. Jiang, Y. Zhang, S. V. Dubonos, I. V. Grigorieva and A. A. Firsov, *Science*, 2004, **306**, 666–669.
2 Z. Chen, J. Wang, D. Pan, Y. Wang, R. Noetzel, H. Li, P. Xie, W. Pei, A. Umar, L. Jiang, N. Li, N. F. Rooij and G. Zhou, *ACS Nano*, 2018, **12**, 2521–2530.

3 G. Fiori, F. Bonaccorso, G. Iannaccone, T. Palacios, D. Neumaier, A. Seabaugh, S. K. Banerjee and L. Colombo, *Nat. Nanotechnol.*, 2014, **9**, 768–779.
4 Y. H. Kim, S. J. Kim, Y. J. Kim, Y. S. Shim, S. Y. Kim, B. H. Hong and H. W. Jang, *ACS Nano*, 2015, **9**, 10453–10460.
5 Y. H. Kim, J. S. Park, Y.-R. Choi, S. Y. Park, S. Y. Lee, W. Sohn, Y.-S. Shim, J.-H. Lee, C. R. Park, Y. S. Choi, B. H. Hong, J. H. Lee, W. H. Lee, D. Lee and H. W. Jang, *J. Mater. Chem. A*, 2017, **5**, 19116–19125.
6 R. Mas-Balleste, C. Gomez-Navarro, J. Gomez-Herrero and F. Zamora, *Nanoscale*, 2011, **3**, 20–30.
7 K. S. Novoselov, A. Mishchenko, A. Carvalho and A. H. Castro Neto, *Science*, 2016, **353**, aac9439.
8 Z. Sun, T. Liao, Y. Dou, S. M. Hwang, M. S. Park, L. Jiang, J. H. Kim and S. X. Dou, *Nat. Commun.*, 2014, **5**, 3813.
9 F. Torrisi and J. N. Coleman, *Nat. Nanotechnol.*, 2014, **9**, 738–739.
10 J. K. Huang, J. Pu, C. L. Hsu, M. H. Chiu, Z. Y. Juang, Y. H. Chang, W. H. Chang, Y. Iwasa, T. Takenobu and L. J. Li, *ACS Nano*, 2014, **8**, 923–930.
11 S. Manzeli, D. Ovchinnikov, D. Pasquier, O. V. Yazyev and A. Kis, *Nat. Rev. Mater.*, 2017, **2**, 17033.
12 C. Tan, Z. Lai and H. Zhang, *Adv. Mater.*, 2017, **29**, 1701392.
13 J. Wang, Y. Wei, H. Li, X. Huang and H. Zhang, *Sci. China Chem.*, 2018, **61**, 1227–1242.
14 X. Zhang, Z. Lai, Q. Ma and H. Zhang, *Chem. Soc. Rev.*, 2018, **47**, 3301–3338.
15 A. Y. Lu, H. Zhu, J. Xiao, C. P. Chuu, Y. Han, M. H. Chiu, C. C. Cheng, C. W. Yang, K. H. Wei, Y. Yang, Y. Wang, D. Sokaras, D. Nordlund, P. Yang, D. A. Muller, M. Y. Chou, X. Zhang and L. J. Li, *Nat. Nanotechnol.*, 2017, **12**, 744–749.
16 J. Zhang, S. Jia, I. Kholmanov, L. Dong, D. Er, W. Chen, H. Guo, Z. Jin, V. B. Shenoy, L. Shi and J. Lou, *ACS Nano*, 2017, **11**, 8192–8198.
17 R. McWeeny, *Rev. Mod. Phys.*, 1960, **32**, 335–369.
18 W. Shi, Z. Wang and Y. Q. Fu, *J. Phys. D: Appl. Phys.*, 2017, **50**, 405303.
19 B. Radisavljevic, A. Radenovic, J. Brivio, V. Giacometti and A. Kis, *Nat. Nanotechnol.*, 2011, **6**, 147–150.
20 E. Gourmelon, O. Lignier, H. Hadouda, G. Couturier, J. C. Bernède, J. Tedd, J. Pouzet and J. Salardenne, *Sol. Energy Mater. Sol. Cells*, 1997, **46**, 115–121.
21 A. Shokri and N. Salami, *Sensor. Actuator. B Chem.*, 2016, **236**, 378–385.
22 R. Chaurasiya and A. Dixit, *Appl. Surf. Sci.*, 2019, **490**, 204–219.
23 R. Chaurasiya and A. Dixit, *Phys. Chem. Chem. Phys.*, 2020, **22**, 13903–13922.
24 C. Jin, X. Tang, X. Tan, S. C. Smith, Y. Dai and L. Kou, *J. Mater. Chem. A*, 2019, **7**, 1099–1106.
25 X.-Y. Yang, T. Hussain, J. P. A. Wärnå, Z. Xu and R. Ahuja, *Comput. Mater. Sci.*, 2021, 186.
26 C. H. Yeh, *ACS Omega*, 2020, **5**, 31398–31406.
27 B. Zhu, K. Zheng, X. Chen, J. Qiu, H. Guo, F. Zhang, L. Lang, J. Yu and J. Bao, *Phys. Chem. Chem. Phys.*, 2021, **23**, 1675–1683.
28 P. Panigrahi, D. Jini, H. Bae, H. Lee, R. Ahuja and T. Hussain, *Appl. Surf. Sci.*, 2021, 542.
29 D. Chen, X. Lei, Y. Wang, S. Zhong, G. Liu, B. Xu and C. Ouyang, *Appl. Surf. Sci.*, 2019, 497.
30 F. Li, W. Wei, H. Wang, B. Huang, Y. Dai and T. Jacob, *J. Phys. Chem. Lett.*, 2019, **10**, 559–565.
31 J. Zeng, G. Liu, Y. Han, W. Luo, M. Wu, B. Xu and C. Ouyang, *ACS Omega*, 2021, **6**, 14639–14647.
32 R. Zhao, T. Wang, M. Zhao, C. Xia, Y. An, S. Wei and X. Dai, *Appl. Surf. Sci.*, 2019, **491**, 128–137.
33 A. C. Aragones, N. L. Haworth, N. Darwish, S. Ciampi, N. J. Bloomfield, G. G. Wallace, I. Diez-Perez and M. L. Coote, *Nature*, 2016, **531**, 88–91.
34 K.-Y. Lin, S. Nachimuthu, M. T. Nguyen, H. Mizuta and J.-C. Jiang, *J. Phys. Chem. C*, 2019, **123**, 30373–30381.
35 S. Nachimuthu, L. He, H.-J. Cheng, R. D. Tiono and J.-C. Jiang, *Sustain. Energy Fuels*, 2021, **5**, 2159–2168.
36 C.-H. Yeh, T. M. L. Pham, S. Nachimuthu and J.-C. Jiang, *ACS Catal.*, 2019, **9**, 8230–8242.
37 L. Yue, N. Wang, S. Zhou, X. Sun, M. Schlangen and H. Schwarz, *Angew. Chem., Int. Ed.*, 2018, **57**, 14635–14639.
38 F. Che, J. T. Gray, S. Ha, N. Kruse, S. L. Scott and J.-S. McEwen, *ACS Catal.*, 2018, **8**, 5153–5174.
39 T. Yabe, K. Yamada, T. Oguri, T. Higo, S. Ogo and Y. Sekine, *ACS Catal.*, 2018, **8**, 11470–11477.
40 N. Sathishkumar, S.-Y. Wu and H.-T. Chen, *Chem. Eng. J.*, 2020, 391.
41 N. Sathishkumar, S.-Y. Wu and H.-T. Chen, *Chem. Eng. J.*, 2021, 407.
42 S. Ma, D. Yuan, Z. Jiao, T. Wang and X. Dai, *J. Phys. Chem. C*, 2017, **121**, 24077–24084.
43 Q. Yue, Z. Shao, S. Chang and J. Li, *Nanoscale Res. Lett.*, 2013, **8**, 425.
44 G. Kresse and J. Hafner, *Phys. Rev. B: Condens. Matter Mater. Phys.*, 1993, **47**, 558–561.
45 G. Kresse and J. Hafner, *Phys. Rev. B: Condens. Matter Mater. Phys.*, 1994, **49**, 14251–14269.
46 G. Kresse and J. Furthmuller, *Phys. Rev. B: Condens. Matter Mater. Phys.*, 1996, **54**, 11169–11186.
47 G. Kresse and J. Furthmüller, *Comput. Mater. Sci.*, 1996, **6**, 15–50.
48 P. E. Blochl, *Phys. Rev. B: Condens. Matter Mater. Phys.*, 1994, **50**, 17953–17979.
49 G. Kresse and D. Joubert, *Phys. Rev. B: Condens. Matter Mater. Phys.*, 1999, **59**, 1758–1775.
50 J. P. Perdew, K. Burke and M. Ernzerhof, *Phys. Rev. Lett.*, 1996, **77**, 3865–3868.
51 H. J. Monkhorst and J. D. Pack, *Phys. Rev. B: Solid State*, 1976, **13**, 5188–5192.
52 S. Grimme, J. Antony, S. Ehrlich and H. Krieg, *J. Chem. Phys.*, 2010, **132**, 154104.
53 S. Grimme, S. Ehrlich and L. Goerigk, *J. Comput. Chem.*, 2011, **32**, 1456–1465.
54 N. G. Limas and T. A. Manz, *RSC Adv.*, 2016, **6**, 45727–45747.
55 T. A. Manz, *RSC Adv.*, 2017, **7**, 45552–45581.
56 T. A. Manz and N. G. Limas, *RSC Adv.*, 2016, **6**, 47771–47801.

57 J. Neugebauer and M. Scheffler, *Phys. Rev. B: Condens. Matter Mater. Phys.*, 1992, **46**, 16067–16080.
58 P. J. Feibelman, *Phys. Rev. B: Condens. Matter Mater. Phys.*, 2001, **64**, 125403.
59 F. Che, J. T. Gray, S. Ha and J.-S. McEwen, *J. Catal.*, 2015, **332**, 187–200.
60 A. Taufik, Y. Asakura, T. Hasegawa and S. Yin, *ACS Appl. Nano Mater.*, 2021, **4**, 6861–6871.
61 K. B. Oldham, *J. Electroanal. Chem.*, 2008, **613**, 131–138.
62 J. S. Filhol and M. L. Doublet, *J. Phys. Chem. C*, 2014, **118**, 19023–19031.
63 E. Masumian, S. M. Hashemianzadeh and A. Nowroozi, *Phys. Lett. A*, 2014, **378**, 2549–2552.
64 I. A. Filot, R. A. van Santen and E. J. Hensen, *Angew. Chem., Int. Ed.*, 2014, **53**, 12746–12750.